Open-boundary cluster model implemented in first-principles calculations for electronic excited states of an adsorbate-surface system

Tomokazu Yasuike and Katsuyuki Nobusada*

Institute for Molecular Science and The Graduate University for Advanced Studies (SOKENDAI), Myodaiji, Okazaki, Aichi 444-8585, Japan

(Received 28 August 2011; published 8 December 2011)

Our recently developed open-boundary cluster model (OCM), which allows us to calculate electronic states of a semi-infinite adsorbate-surface system with a finite-small cluster, has been implemented in first-principles calculations to investigate excited states of a real system of a low-coverage Cs/Cu(111). The first-principles calculations are based on a real-space density functional theory (DFT) approach, and the Cs/Cu(111) system is reasonably represented in terms of a cluster of $CsCu_{13}$ within the OCM approach. An absorption spectrum and the lifetime of excited states of the system are calculated successfully within the linear-response approximation, and the computed results qualitatively agree with experimental observations. Such excited properties are difficult to calculate by using a conventional cluster model (CCM) approach. Despite these advantages, the OCM-DFT approach requires a computational cost almost identical to the cost of CCM.

DOI: 10.1103/PhysRevB.84.245408 PACS number(s): 73.20.Hb, 68.43.−h, 71.15.Qe

I. INTRODUCTION

Recently, the importance of photoexcited interfacial processes has been growing rapidly.[1,2] These processes play an essential role not only in basic chemicophysical science, but also in their relevance to a broad range of practical applications to dye-sensitized solar cells,[3] photocatalysts,[4,5] artificial photosynthesis,[6] imaging,[7] and organic semiconductor-based photovoltaics.[8] To investigate photoexcited interfacial systems, it is crucial to understand electronic excited states of adsorbate-metal or adsorbate-semi-conductor surface systems. According to the Newns-Anderson theory,[9] the electronic state localized on an adsorbate interacts with surface continuum states and forms a resonance state[10] with a complex-valued eigenenergy. The imaginary part represents the decay rate of the excited state in the region near the adsorbate and corresponds physically to the irreversible electron transfer rate from the adsorbate to the substrate. The interfacial electron transfer occurring from an adsorbate excited state is a key process to determine the overall efficiency of photoexcited interfacial processes, for example, in dye-sensitized solar cells.[3] Despite its great technological significance, fundamental understanding of the interfacial electron transfer remains unresolved. The rate of interfacial electron transfer is known to be on the order of femtoseconds for many systems.[11,12] The nuclear motion cannot be a rate-determining factor in the interfacial electron transfer, unlike the electron transfer in homogeneous solutions where the nuclear reorganization process plays important roles. The electron dynamics has a direct importance, and developing a theoretical method capable of describing the resonance state in adsorbate-metal and adsorbate-semiconductor surface systems is highly desirable.

Since the conventional cluster model (CCM) and slab model approaches only give real eigenenergies, the approaches do not describe adsorbate electronic excited states interacting with metal or semiconductor surfaces appropriately. In that sense, the most reliable method at the present time is an embedded cluster model where the surface effect is described by using the surface Green function (sGF).[13–18] However, this approach gives an energy-dependent effective Hamiltonian and so far, has not been used widely. Recently, we have developed the open-boundary cluster model (OCM) approach.[19–21] This is a simple alternative to the embedded cluster model. A model cluster is embedded effectively by introducing the physically meaningful outgoing-wave boundary condition at the edge of the cluster. The resultant Hamiltonian is energy independent and is a good approximation to one obtained by the sGF-based embedding theory. The OCM approach also is a generalization of Nordlander-Tully's treatment[22] of adsorbate-jellium surfaces by using the complex-scaling technique.

The CCM approach is known to fail to describe covalent adsorptions on metal surfaces and gives a severe cluster-size dependence of computed properties,[23,24] whereas, it gives a good description for insulating surfaces[25] and alkali adsorption on metal surfaces.[26–28] For simple model systems, we have demonstrated that the OCM approach significantly reduces the cluster-size dependence of computed properties and has a general applicability without depending on the character of adsorption. Most noteworthy is that the OCM approach enables us to easily calculate excitation energies as well as electron-transfer rates for electronic excited states. Also, we have shown that the adsorbate excited states are decoupled from the infinite number of intrabulk excited states,[20] and we are able to easily treat chemical reactions in photoexcited interfacial species at a low computational cost.[21] Both potential-energy curves and electron-transfer rates for excited states are required for understanding photoexcited interfacial processes, and thus, the OCM approach is considered to be one of the most promising methods.

In the present paper, we implement our OCM approach in first-principles calculations based on the real-space density functional theory (DFT)[29,30] to investigate Cs/Cu(111) as a real adsorbate-surface system. This system is ideal for the first application because a great deal of information is known about its excited states, and the adsorption has an ionic-bonding character easily treatable with a cluster model.

II. METHODS

A. DFT calculations with the OCM

The OCM Hamiltonian is constructed by introducing the outgoing-wave boundary condition (OBC) at the edge of

a model cluster. The complex-scaling technique is most appropriate for this purpose, and thus, we have employed the technique for a model one-body system in our original paper.[19] However, the integration of this technique into the DFT formalism has not been established well. In the present paper, we alternatively introduce the OBC by adding a pure imaginary absorbing potential $-i\,v_{\rm abs}(z)$ to the CCM Hamiltonian. Then, the Kohn-Sham (KS) equation[31] is given by

$$\left(-\frac{1}{2}\nabla^2 + v(\boldsymbol{r}) + \int \frac{\rho(\boldsymbol{r}')}{|\boldsymbol{r}-\boldsymbol{r}'|}d\boldsymbol{r}' + v_{\rm XC}(\boldsymbol{r}) - i\,v_{\rm abs}(z)\right) \phi_i(\boldsymbol{r}) = \epsilon_i\phi_i(\boldsymbol{r}), \tag{1}$$

where $v(\boldsymbol{r})$, $\rho(\boldsymbol{r})$, and $v_{\rm XC}(\boldsymbol{r})$ are the nuclear attraction potential, the electron density, and the exchange-correlation functional, respectively. The absorbing potential is employed to meet the outgoing boundary condition along the z direction normal to the surface so that the semi-infiniteness in this direction of an adsorbate-surface system is described appropriately. The explicit function form of $v_{\rm abs}(z)$ for $-z_2 \leqslant z < -z_1$ is

$$-i\,v_{\rm abs}(z) = -i\left(\frac{2\pi}{c w_{\rm ab}}\right)^2 \left\{ \frac{2}{\left(1-\frac{z-z_1}{w_{\rm ab}}\right)^2} + \frac{2}{\left(1+\frac{z-z_1}{w_{\rm ab}}\right)^2} - 4 \right\}, \tag{2}$$

where c is $2\sqrt{\pi}\Gamma(5/4)/\Gamma(3/4)$ and $w_{\rm ab} = |z_2 - z_1|$. This form was proposed by Manolopoulos and co-workers[32,33] and was specified by a single physical parameter, the width of the absorbing region $w_{\rm ab}$. The value of $-z_2$ is set to the bound of the calculation box, and $w_{\rm ab}$ is replaced by the scaled $w'_{\rm ab} \equiv 1.125 w_{\rm ab}$ to avoid the divergence of $v_{\rm abs}(-z_2)$.

The orbital energies ϵ_i become complex, $\epsilon_i = e_i - i\gamma_i/2$, owing to the imaginary potential. The corresponding one-body density of states is given by a Lorentzian function,

$$n_i(\epsilon) = \frac{1}{\pi}\frac{\gamma_i/2}{(\epsilon - e_i)^2 + (\gamma_i/2)^2}, \tag{3}$$

and the occupation number is determined by the chemical potential μ as follows:

$$n_i = 2\int_{-\infty}^{\mu} n_i(\epsilon)d\epsilon = 1 - \frac{2}{\pi}\arctan\left[\frac{2(\mu - e_i)}{\gamma_i}\right]. \tag{4}$$

Then, the occupation number n_i of each orbital is fractional in general. The chemical potential is more appropriate than the total number of electrons to define a system interacting with continuum states because the total number of electrons is not defined uniquely for bulk materials. It reflects that the OCM approach is suitable for describing an adsorbate interacting with a bulk material.

The orbitals determined by a complex symmetric Fock matrix are orthonormalized by not using the Hermite norm but the c product[34] defined without the complex conjugation of the bra state in the inner product. Therefore, from the viewpoint of the normalization of the existing probability, the electron density should not be defined by the squared absolute values of the orbitals, $|\psi_i(\boldsymbol{r})|^2$ but by the the real parts of the squared orbitals $\psi_i(\boldsymbol{r})^2$,

$$\rho(\boldsymbol{r}) = \sum_i n_i {\rm Re}[\psi_i(\boldsymbol{r})^2]. \tag{5}$$

The use of the Hermite norm definition for phenomena relating to resonance[35,36] was criticized by Ernzerhof,[37] and he proposed the direct use of the complex electron density $\sum_i n_i\psi_i(\boldsymbol{r})^2$. However, the complex electron density causes severe instabilities in practical applications. According to Berggren,[38] the quantity on the right-hand side of Eq. (5) is interpreted as the expectation value of electron density, and it is a reasonable choice to avoid computational instability due to the variableness of exchange-correlation functional $v_{\rm XC}$. The calculations employing Eq. (5) are highly stable.

B. Excited states

Excited states of adsorbate-surface systems are obtained by calculating the linear response of the ground state. The linear-response theory for a fractional-occupation number (FON) state has been formulated independently by Jørgensen[39] and Casida[40] within the frameworks of Hartree-Fock and DFT approaches, respectively. Their formulations are generalized straightforwardly for the complex-valued symmetric case by

$$\begin{pmatrix} \mathbf{A} & \mathbf{B} \\ \mathbf{B} & \mathbf{A} \end{pmatrix}\begin{pmatrix} \mathbf{X}^n \\ \mathbf{Y}^n \end{pmatrix} = \omega_n \begin{pmatrix} \boldsymbol{\lambda} & \mathbf{0} \\ \mathbf{0} & -\boldsymbol{\lambda} \end{pmatrix}\begin{pmatrix} \mathbf{X}^n \\ \mathbf{Y}^n \end{pmatrix}, \tag{6}$$

where $\mathbf{X}^n$ and $\mathbf{Y}^n$ vectors are formed by collecting the amplitudes for particle-hole (p-h) and hole-particle (h-p) pair excitations, respectively, in the KS orbital representation. The matrix elements of $\mathbf{A}$, $\mathbf{B}$, and $\boldsymbol{\lambda}$ are

$$A_{ia,jb} = (n_i - n_a)\{\epsilon_a - {\rm Re}(\epsilon_i)\}\delta_{ij}\delta_{ab} + (n_i - n_a)(n_j - n_b)K_{ia,jb}, \tag{7}$$

$$B_{ia,jb} = (n_i - n_a)(n_j - n_b)K_{ia,jb}, \tag{8}$$

$$\lambda_{ia,jb} = (n_i - n_a)(n_j - n_b)\delta_{ij}\delta_{ab}, \tag{9}$$

where

$$K_{ia,jb} = \int d\mathbf{r}\,d\mathbf{r}'\phi_i(\mathbf{r})\phi_a(\mathbf{r})\left[\frac{1}{|\mathbf{r}-\mathbf{r}'|} + \frac{\delta v_{\rm XC}(\rho)}{\delta\rho}\delta(\mathbf{r}-\mathbf{r}')\right] \times \phi_b(\mathbf{r}')\phi_j(\mathbf{r}'). \tag{10}$$

The indices i,j and a,b denote occupied (hole) and vacant (particle) orbitals, respectively. Since the occupation numbers are fractional, it is difficult to distinguish between occupied and vacant orbitals in terms of the occupation number. In the FON-state-based linear-response theory, however, the hole-particle excitations having a positive value of $n_i - n_a$ are taken into account, and thus, the occupied and vacant orbitals are defined by the orbitals having larger and smaller occupation numbers, respectively. The real part of the complex-valued ϵ_i is adopted for defining Eq. (7) because the dissipation from the occupied orbital should be canceled by the backward electron transfer in the equilibrium, i.e., the ground state.[19]

From the specific form of the working equation given by Eq. (6), the orthonormality relation between eigenvectors is given by

$$\sum_{ia}\left(X^n_{ia}X^m_{ia} - Y^n_{ia}Y^m_{ia}\right) = \delta_{n,m}. \tag{11}$$

The electric transition dipole moment μ_{0n} of the excitation from $|\Psi_0\rangle$ to $|\Psi_n\rangle$ is obtained by

$$\mu_{0n} = (\Psi_0|\hat{\mu}|\Psi_n) = \sum_{ia} \sqrt{2}\left(X^n_{ia}\mu_{ia} + Y^n_{ia}\mu_{ia}\right), \quad (12)$$

where $\hat{\mu} \equiv -\mathbf{r}$ and $\mu_{ia} \equiv \int \phi_i(\mathbf{r})\hat{\mu}\phi_a(\mathbf{r})d\mathbf{r}$. The quantity μ_{ia} is the transition dipole moment for the individual excitation of $\phi_i \rightarrow \phi_a$. The round bracket indicates the c product, and the real part of μ_{0n} is the expectation value of the transition dipole moment.

C. Computational details

To investigate excited states of a Cs/Cu(111) system, we carry out the first-principles OCM calculations of $CsCu_n$ (n = 1, 7, 10, 13, 19, and 31). In these models, the substrate Cu_n clusters are sections of the ideal Cu(111) surface where the Cu-Cu and interlayer distances are 2.553 and 2.084 Å, respectively. The adsorption of the Cs atom is known to occur on the on-top site for the Cu(111) surface at the coverage of 0.25 monolayer (ML).[41] We assume the on-top site adsorption for the low-coverage limit considered in the present paper. The minimal model cluster is a diatomic CsCu molecule. $CsCu_7$ is a cluster model with an adsorbate atom Cs centered on a single layer consisting of seven copper atoms. As double-layer models, we consider $CsCu_{10}^{(7/3)}$ and $CsCu_{13}^{(7/6)}$ clusters, where the numbers i and j of (i/j) indicate the number of Cu atoms in the first and second layers, respectively. The triple-layer models employed are $CsCu_{19}^{(7/6/6)}$ and $CsCu_{31}^{(7/12/12)}$.

The cesium and copper atoms are described by the norm-conserving pseudopotential,[42] and only 6s and 4s electrons, respectively, are considered explicitly in the calculations. We concentrate on the low-lying excited states where only the sp-band excitation of the substrate is essential, and the copper 3d electrons are treated as frozen core electrons. The three-dimensional uniform grids are used for the spatial representation. The employed grid size is 0.4 Å, and this is reasonable for Cu 4sp and Cs 6sp5d electrons. The computational box size is $20 \times 20 \times 20$ Å, and the total number of grid points is 125000. The local density approximation[43] is employed for v_{XC}. For some clusters, the self-consistent field (SCF) calculations showed a poor convergence, and thus, the Anderson mixing method[44] was employed for the electron-density update in the SCF cycle. All the calculations are carried out by using our developed program based on the real-space grid DFT method.

III. RESULTS AND DISCUSSION

A. Optimization of absorbing potential

The absorbing potential is employed to practically represent the OBC. Thus, the potential is determined so that the computed resonance energies are invariant for the choice of potential. However, the results often show a non-negligible dependence on the potential. The optimization of the absorbing potential is required on the basis of the local stability of the computed energy on absorbing-potential parameters.[34] Since the absorbing potential employed in the present paper only has one parameter, the absorbing width w_{ab}, it is easy to optimize the potential without ambiguity.

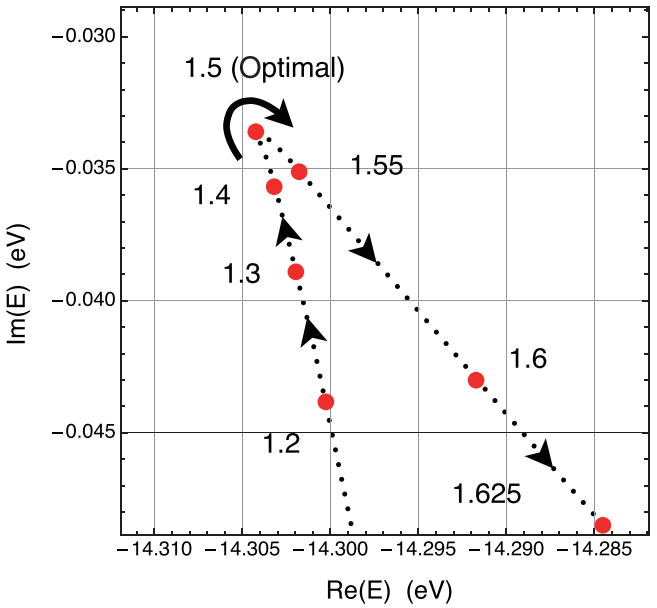

FIG. 1. (Color online) Absorbing-potential dependence of the complex energy for the ground state of CsCu. The numbers indicate the values of parameter w_{ab} defining the absorbing potential for each calculation. The cusp structure seen at $w_{ab} = 1.5a_0$ indicates a stability in the energy eigenvalue at this value of w_{ab}. From the view of the variational principle of resonance states, the absorbing potential with $w_{ab} = 1.5a_0$ is found to be optimal.

We calculated the KS total energy for the ground state of CsCu for various values of w_{ab}. The substrate Cu atom is located at $z = -7.0a_0$. Figure 1 shows the eigenenergy trajectory on the complex-energy plane. The trajectory shows a cusp near $w_{ab} = 1.5a_0$, and the eigenenergy slowly varies near the cusp. Therefore, the absorbing potential with $w_{ab} = 1.5a_0$ is optimal for the electronic ground states of CsCu. From the orbital-energy trajectories, the cusp of the total-energy trajectory is due to the fact that all the orbital energies show the cusp at $w_{ab} = 1.5a_0$. For this reason, the optimal value is independent of their occupation numbers. In other words, the optimal value of w_{ab} is common to all the electronic states distinguished by the occupation numbers. Furthermore, the orbital-energy trajectories were found to have cusps for the same w_{ab} irrespective of the size and geometry of the clusters, if the grid spacings adopted are the same. In this sense, the absorbing potential optimized for a cluster is universal for different clusters and electronic states. We, thus, employed the absorbing potential with $w_{ab} = 1.5a_0$ in all the following calculations.

B. Cluster-size dependence

The intensive studies by Bagus and co-workers[26–28] have shown that the CCM approach gives a reasonable description of the ground-state properties for ionic adsorption of alkali metals on transition-metal surfaces if the substrate is modeled by a cluster with an appropriate size. We first checked the cluster-size dependence of the calculated properties. Figure 2(a) is the cluster-size dependence of the Fermi energy of the substrate Cu clusters. The overall behavior is similar between the results obtained by the CCM and OCM approaches. The OCM result is almost converged at $n \geqslant 13$,

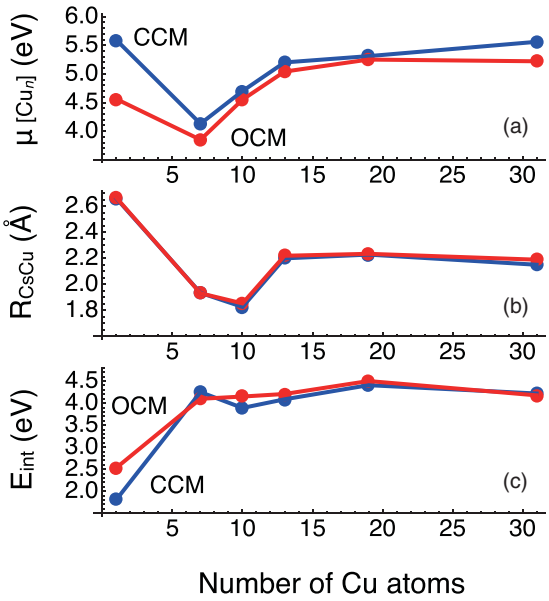

FIG. 2. (Color online) Cluster-size dependences of (a) the Fermi energy of the substrate Cu_n cluster, (b) the equilibrium Cs-Cu distance, and (c) the interaction energy between Cs and Cu_n clusters. The red and blue lines indicate the OCM and CCM results, respectively. All figures show that reasonable convergence has been obtained already for the substrate cluster of Cu_{13}.

and its energy is close to 4.9 eV, the experimental Fermi energy of the clean Cu(111) surface. It should be noted that the CCM Cu_{31} cluster still is not converged well.

The equilibrium adsorption distance shown in Fig. 2(b) also is converged at $n \geqslant 13$. The geometry is known to be calculated more easily even by the CCM approach.

Figure 2(c) shows the cluster-size dependence of the interaction energy $E_{\rm int}$ defined as

$$E_{\rm int} = E(\mathrm{CsCu}_n) - E(\mathrm{Cu}_n) - E(\mathrm{Cs}), \qquad (13)$$

where $E(\mathrm{CsCu}_n)$, $E(\mathrm{Cu}_n)$, and $E(\mathrm{Cs})$ are the total energies of CsCu_n, Cu_n, and Cs, respectively. The interaction energy generally is known to show a slow convergence with the cluster size. For example, those of the covalent adsorption, such as H/Ni(100) (Ref. 23), H/Ni(111) (Ref. 23), and CO/Cu(100) (Ref. 24) show significant oscillating behavior depending on the cluster size. In contrast, as shown by Siehbahn *et al.*,[45] the interaction-energy oscillation is much weaker for the ionic adsorption. The adsorption in the Cs/Cu(111) system would be ionic, and thus, the CCM approach is expected to give a reasonable result. The CCM result shown in Fig. 2(c) actually gives a relatively smooth convergence with a small oscillation. The OCM approach further reduces this small oscillation. It is expected that the OCM approach well reproduces electronic properties even in the systems where the covalent-bonding character is essential.

C. Minimal cluster model of Cs/Cu(111)

From the cluster-size dependence described above, the diatomic CsCu model is not suitable for representing Cs/Cu(111). More specifically, its interaction energy is underestimated, whereas, the adsorption distance is overestimated. This is understood qualitatively in terms of the low-electron acceptance ability of Cu. In addition to its low-electron affinity (1.23 eV), the Cu atom has a polarizability much smaller than that of the bulk Cu. Thus, the surface-image charge in the Cu(111) surface would not be represented appropriately. For this limited acceptance ability of an electron, the ionic character in the Cs-Cu bonding is expected to be underestimated. It leads to the smaller $E_{\rm int}$ and the larger $R_{\rm CsCu}$. This explanation can be confirmed by analyzing the dipole moment curves. The dipole moment in the z direction of the surface normal is calculated by

$$\mu_z = \sum_A Z_A z_A + \sum_i n_i \int \phi_i(\boldsymbol{r})(-ez_i)\phi_i(\boldsymbol{r})d\boldsymbol{r}, \qquad (14)$$

where Z_A is the nuclear charge and z_A and z_i are the z coordinates of the nucleus and the electron, respectively. Figures 3(a) and 3(b) show the dipole moment curves for CuCs and $Cu_{13}Cs$, respectively. The expansion of μ_z about the equilibrium $R_{\rm CsCu}$ is

$$\mu_z\left(R^{\rm eq}_{\rm CsCu}\right) = \mu^{\rm eq}_z + M_1\left(R_{\rm CsCu} - R^{\rm eq}_{\rm CsCu}\right) + \cdots, \qquad (15)$$

where $M_1 = d\mu_z/dR_{\rm CsCu}$. The value of M_1 is an index to measure the bonding nature of Cs adsorbed on the Cu substrate clusters. For an ideal ionic adsorbate with charge +1 and without any polarization, $M_1 = 1$.[27] The $CsCu_{13}$ cluster actually gives $M_1 = 1.02$, and the adsorption is purely ionic. In contrast, the diatomic CsCu gives $M_1 = -0.13$. This value is small and typical of a covalent bond. Therefore, the failure of the diatomic CsCu model is attributed to the poor description of the ionic character of the bonding. For these reasons, we

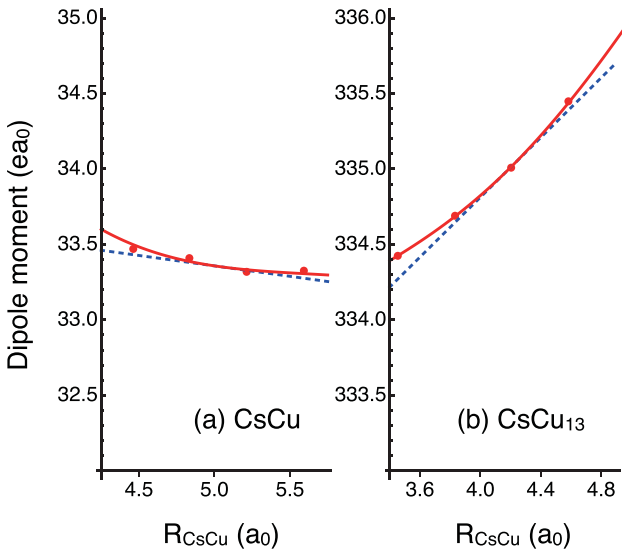

FIG. 3. (Color online) Adsorption-distance ($R_{\rm CsCu}$) dependences of the electric dipole moment of (a) CsCu and (b) $CsCu_{13}$. The blue-dotted line is tangent to the dipole moment curve (red) at the equilibrium adsorption distance. Its slope is an index for ionicity in the adsorption bond. The actual slope values are −0.13 and +1.02 for CsCu and $CsCu_{13}$, respectively. These values imply that the Cs atom is neutral in CsCu and is cationic in $CsCu_{13}$. The $CsCu_{13}$ cluster is more appropriate for mimicking purely cationic Cs atoms in the low-coverage limit of Cs/Cu(111).

TABLE I. Peak positions and lifetimes of Cu(111) and Cs/Cu(111) systems.

System	Peak position and lifetime			
Cu(111) Experiment				4.1 eV (Refs. 46–48) 10 ± 3 fs (Ref. 49)
Cu_{13}[a]				4.06 eV 11 fs
Cs/Cu(111) Experiment		∼3.0 eV (Refs. 51–54) 50 fs (Ref. 54) 15 ± 6 fs (Ref. 52)		∼4.0 eV (Ref. 53)
CsCu[a]	2.56 eV 55 fs	2.95 eV 112 fs	3.54 eV 134 fs	4.16 eV 58 fs
$CsCu_{13}$[a]		2.95 eV 42 fs		3.90 eV 20 fs

[a]Present results.

concluded that $CsCu_{13}$ is the minimal model for representing the low-coverage limit of the Cs/Cu(111) system.

The above analysis of the adsorption character explains the reason for the equilibrium adsorption distance of $CsCu_{13}$ (2.22 Å) being much smaller than the experimental value (3.01 Å). This is because the experimental value was determined under the high-coverage (0.25-ML) condition with the $p(2 \times 2)$ structure, whereas, the cluster model represents the system at the low-coverage limit. For alkali adsorbates on transition-metal surfaces, the bonding nature is known to depend on the coverage. Under the low-coverage condition, the bond is purely ionic, and it becomes covalent with increasing the coverage. With the full coverage, the Cs layer finally becomes metallic and shows a plasmonic response. Then, under the high-coverage experimental condition, the adsorption is covalent, and the adsorption distance is different from that of the ionic adsorption at the low-coverage limit. In this sense, the covalent CsCu diatomic molecule partially represents the high-coverage situation, and it is reasonable that the CsCu adsorption distance of 2.66 Å is closer to the experimental value of 3.01 Å. This is understood intuitively because the ratio of the adsorbate and substrate atoms in CsCu is higher than in $CsCu_{13}$.

D. Previous assignment and computed photoabsorption spectrum of CsCu

The excited states of the Cu(111) and Cs/Cu(111) systems have been investigated intensively. For the clean Cu(111) surface, it has been revealed by the two-photon photoemission (2PPE)[46] and inverse photoemission (IPE)[47] spectroscopies that there is an excited state at around 4.1 eV. The resonant enhancement of the second-harmonic generation for the photon energy, which is half of 4.1 eV, has been reported by Lüpke *et al.*[48] The electronic lifetime of this state has been determined as 10 ± 3 fs by the time-resolved 2PPE spectroscopy.[49] This state is known to be formed by the excitation from the surface state to the image-potential state with the quantum number of $n = 1$.[50] Due to the Cs adsorption, Cs-induced peaks arise. The lowest one is at ~ 3.0 eV for the low-coverage limit.[51–54] This state was widely thought to be the Cs $6s$ resonance, whereas, the possibility of the Cs $5d$ contribution was pointed out by Arena *et al.*[53] The experimentally observed lifetimes of this state are 15 ± 6 fs (Ref. 52) and 50 fs,[54] depending on temperature. These main features of the excited states of Cu(111) and Cs/Cu(111) are summarized in Table I.

Theoretically, Borisov *et al.* have estimated[55] the lifetime to be 28 fs for the lowest σ state of Cs/Cu(111) by using a one-dimensional model potential for Cu(111). In their treatment of electron-surface interaction, only the modulation of the potential along the surface normal was considered, and a free-electron motion parallel to the surface was assumed. Their treatment is similar to the diatomic CsCu model in the sense that no Cu atoms around the Cs-adsorbed Cu atom were taken into account.

Figure 4(a) shows the computed photoabsorption spectra of CsCu in the framework of the OCM. The spectrum has four sharp peaks, indicated by A, B, C, and D, in the energy region from 2.6 to 4.2 eV. The inset shows the orbitals relevant to the excitations of A and B. Excitations A and B are mainly expressed as the excitations of $\psi_{\rm occ} \rightarrow \psi_{\rm a}$ and $\psi_{\rm occ} \rightarrow \psi_{\rm b}$, respectively. As clearly shown by the orbital shapes of $\psi_{\rm occ}$ and ψ_a, the lowest state A is attributed to the excitation from the substrate to Cs $6sp\sigma$ orbitals. This assignment is the same as the previous ones by Borisov and co-workers[55] and by Nordlander and Tully.[22] However, its excitation energy of 2.56 eV is rather lower than 3.0 eV of the experimental Cs-derived peak,[51–54] and it includes no contribution from Cs $5d$. On the other hand, the B state has the excitation energy of 2.95 eV close to the experimental one and is characterized mainly by Cs $5d\sigma$. However, the absorption strength is too weak to explain the experimental IPE spectrum. Furthermore, the experimental spectrum only shows two sharp peaks in the energy region shown in Fig. 4, and the overall feature of the CsCu spectrum does not correspond to the experiment.[53] We then conclude that the Cu atoms around the Cs-adsorbed Cu atom are needed for reproducing the photoabsorption spectrum.

E. Photoabsorption spectra of $CsCu_{13}$

Figure 4(b) shows the photoabsorption spectrum of $CsCu_{13}$. The spectrum is quite different from that of the CsCu model.

The number of the substrate orbitals increases from CsCu, and many additional excitation peaks appear. Their energy widths are relatively broad, and these states form a continuous background as the cluster size is enlarged further. The $CsCu_{19}$ spectrum shown in Fig. 4(c) shows continuouslike features of the background and gives more quantitative agreement with the IPE spectrum by Arena *et al.*,[53] indicated by the red-dashed curve. However, it should be emphasized that the $CsCu_{13}$ spectrum already reproduces the qualitative feature that there are two sharp peaks at ∼3.0 and ∼4.0 eV apart from the broad background. Thus, $CsCu_{13}$ is regarded as the minimal model of Cs/Cu(111) even for the excited-state properties. We discuss the assignment of these sharp peaks on the basis of the results of $CsCu_{13}$. In Fig. 4(b), two sharp peaks of $CsCu_{13}$ exist at 2.95 and 3.90 eV. The lifetime of the excited state at 2.95 eV is 42 fs and is comparable to the experimental value of 50 fs by Ogawa and co-workers.[54] Figure 5 shows the transition-density distributions (TDDs) for the excitation at 2.95 eV. The upper and lower figures are the top and side views, respectively, of the TDDs. The total TDDs are shown on the left-hand side. As the top view clearly indicates, the radial breathing motion around the Cs-Cu axis is induced by this excitation. Therefore, the present assignment is different qualitatively from those of previous papers[22,55] where it was assigned to the Cs $6sp\sigma$ state. The difference between the present and the previous results is due to the model potential employed for the Cu(111) surface. The previous papers used a potential uniform in the radial direction, whereas, our model explicitly has six Cu atoms around the Cs-adsorbed Cu atom. The breathing mode is stabilized by the outer six Cu atoms, and this mode becomes energetically lower than the excitation related to the Cs $6sp\sigma$ orbital of ψ_{20}. The partial TDD indicated by PI (partial component I) of Fig. 5 mainly contributes to the total one and consists of the excitations of $\psi_5 \rightarrow \psi_{11}$ and $\psi_6 \rightarrow \psi_{12}$. As shown in Fig. 6, the orbitals ψ_{11} and ψ_{12} include Cs $5d\pi$ contributions. The next largest partial TDD, indicated

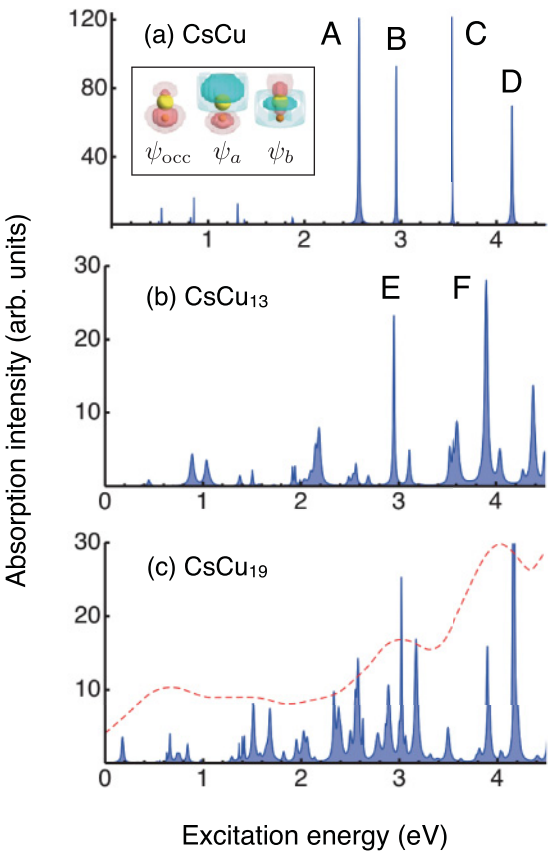

FIG. 4. (Color online) Computed photoabsorption spectra of (a) CsCu, (b) $CsCu_{13}$, and (c) $CsCu_{19}$. The inset shows the occupied and two final orbitals in excitations A and B. The yellow and orange spheres are Cs and Cu atoms, respectively. The pink and blue colors show the isoamplitude surfaces of the orbitals. The dark (light) colors indicate 25 (10)% of the maximal absolute value. The ψ_{occ}, ψ_a, and ψ_b orbitals are assigned to Cu4*s*-Cs6$sp\sigma$ bonding, Cu4*s*-Cs6$sp\sigma$ antibonding, and Cs5$d\sigma$ nonbonding orbitals, respectively. The red-dashed curve of (c) is the experimental IPE spectrum of Cs/Cu(111) at the coverage of 0.04 ML, taken from Ref. 53.

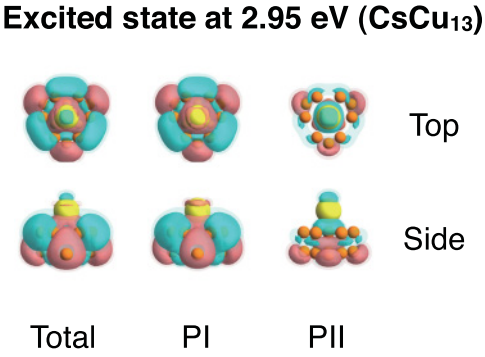

FIG. 5. (Color online) TDD for the excitation at 2.95 eV. The leftmost figures are total TDDs. PI and PII TDDs are for the most and secondary-most important elementary excitations, respectively. The pink and blue colors show the isodensity surfaces. The dark (light) colors indicate 10 (5)% of the maximal absolute value. The excitation at 2.95 eV consists of the intrasubstrate (PI) and the substrate-Cs5$d\sigma$ charge-transfer (PII) excitations.

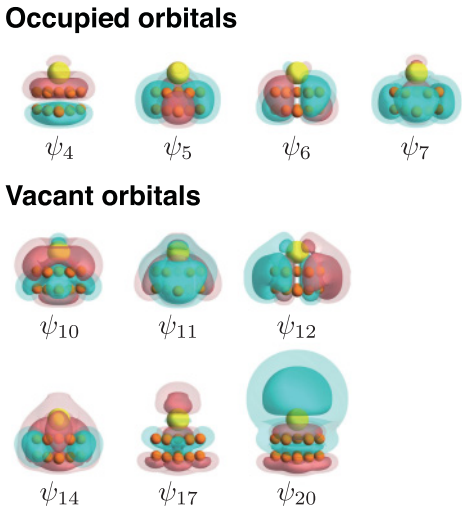

FIG. 6. (Color online) Relevant orbitals for low-lying excitations of $CsCu_{13}$. The yellow and orange spheres are Cs and Cu atoms, respectively. The pink and blue colors show the isoamplitude surfaces of the orbitals. The dark (light) colors indicate 25 (10)% of the maximal absolute value.

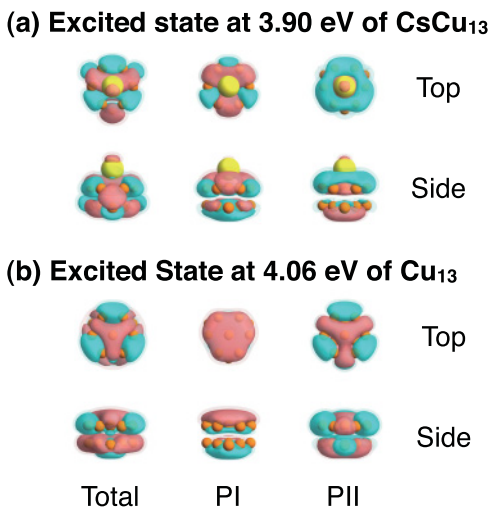

FIG. 7. (Color online) TDDs for the excitations at (a) 3.90 eV of $CsCu_{13}$ and (b) 4.06 eV of Cu_{13}. The leftmost figures are total TDDs. PI and PII TDDs are for the most and secondary-most important elementary excitations, respectively. The pink and blue colors show the isodensity surfaces. The dark (light) colors indicate 10 (5)% of the maximal absolute value. The excitations at 3.90 eV of $CsCu_{13}$ and 4.06 eV of Cu_{13} essentially are equivalent to each other, although the importance of PI and PII is inversed by the Cs adsorption. Both PI and PII excitations are related to interlayer electronic motion.

by PII (partial component II), is formed by the excitation of $\psi_7 \rightarrow \psi_{17}$. The orbital ψ_{17} includes the Cs $5d\sigma$ contribution. These Cs $5d$ contributions are consistent with the experimental observation by Arena *et al.*[53]

Figure 7(a) shows the TDDs for the excitation of $CsCu_{13}$ at 3.90 eV. In addition to the breathing motion, the Cu interlayer oscillation contributes to this excitation. In particular, the PII TDD of $CsCu_{13}$ resembles the PI TDD of Cu_{13} shown in Fig. 7(b). The interlayer oscillation indicated by the PI TDD of the excitation at 4.06 eV of Cu_{13} corresponds to one of the excitations from the surface state to the image potential state ($n = 1$). It is concluded that Cs/Cu(111) has the adsorbate-perturbed Cu interlayer excitation at a slightly lower energy than that of the Cu(111) excitation. The experimental lifetime of the excited state at 4.1 eV of Cu(111) is 10 ± 3 fs, and the computed lifetime of the excitation at 4.06 eV of Cu_{13} is 11 fs. The agreement is excellent, and it is one of the confirmations of the validity of the present calculation.

IV. CONCLUSION

First-principles calculations combined with the OCM approach have been applied to electronic excited states of a Cs/Cu(111) adsorbate-surface system. The OCM approach allows us to reasonably model the semi-infinite Cs/Cu(111) system with a finite-small $CsCu_{13}$ cluster. The analysis based on the dipole moment curve has revealed that the Cs adsorption is purely ionic for the low-coverage limit of Cs adsorption, whereas, the smallest cluster model of CsCu inappropriately represents the Cs adsorption to be a covalent bonding.

The computed photoabsorption spectrum of $CsCu_{13}$ gives good agreement with the experimental IPE spectrum by Arena *et al.*[53] The assignment of the sharp peaks at ~3.0 and 4.0 eV is carried out by analyzing the TDDs and orbitals relevant to the excitations. The analysis concludes that the lower peak has a large contribution from the radial breathing motion of the substrate electrons. This is reasonable because the lower peak is observed strongly even for very small coverage, and the intensity only depends weakly on the coverage.[53] The present assignment is different from previous ones. The reason for that is due to the difference in surface model potentials employed in the calculations. Our cluster model considers the Cu atoms existing around the Cs-adsorbed Cu atom to reproduce a real Cs/Cu(111) system, whereas, a rather simple model potential, that is, uniform potential in the radial direction, was employed in previous papers. The computed lifetime of the state at 2.95 eV is 42 fs comparable to 50 fs observed by Ogawa *et al.*[54] Moreover, the Cs $5d$ contribution in the computed excited state corresponds to the observation by Arena *et al.*[53] The higher-energy peak has been revealed to be reminiscent of the excitation from the surface state to the image-potential state with $n = 1$ of Cu(111). The detailed comparison of the properties obtained by the OCM approach with the experimental evidence clearly demonstrates the validity of our approach. The OCM approach requires a computational cost similar to the cost of the CCM and is a powerful tool for discussing the photoexcited interfacial molecular processes.

ACKNOWLEDGMENTS

The research was supported by a Grant-in-Aid (Grants No. 21350018 and No. 23750028) and by the Next-Generation Supercomputer Project from the Ministry of Education, Culture, Sports, Science and Technology of Japan. We thank Y. Matsumoto and K. Watanabe for helpful discussions and comments regarding the electronic states of Cs/Cu(111).

*Author to whom correspondence should be addressed.

[1] X.-Y. Zhu, J. Phys. Chem. B **108**, 8778 (2004).
[2] C. D. Lindstrom and X.-Y. Zhu, Chem. Rev. **106**, 4281 (2006).
[3] A. Hagfeld and M. Grätzel, Acc. Chem. Res. **33**, 269 (2000).
[4] A. Fujishima and K. Honda, Nature (London) **238**, 37 (1972).
[5] A. L. Linsebigler, G. Lu, and J. T. Yates Jr., Chem. Rev. **95**, 735 (1995).
[6] K. Kalayanasundaram and M. Grätzel, Coord. Chem. Rev. **77**, 347 (1998).
[7] K. Jacobson and R. Jacobson, in *Imaging Systems* (Wiley, New York, 1976).
[8] B. A. Gregg, MRS Bull. **30**, 20 (2005).
[9] D. M. Newns, Phys. Rev. **178**, 1123 (1969).
[10] A. J. F. Siegert, Phys. Rev. **56**, 750 (1939).
[11] J. Schnadt *et al.*, Nature (London) **418**, 620 (2002).
[12] R. Huber, J. E. Moser, M. Grätzel, and J. Wachtveitl, J. Phys. Chem. B **106**, 6494 (2002).
[13] P. Huang and E. A. Carter, Annu. Rev. Phys. Chem. **59**, 261 (2008).

[14]T. B. Grimley and C. Pisani, J. Phys. C **7**, 2831 (1974).
[15]A. R. Williams, P. J. Feibelman, and N. D. Lang, Phys. Rev. B **26**, 5433 (1982).
[16]T. Klamroth and P. Saalfrank, Surf. Sci. **410**, 21 (1998).
[17]J. E. Inglesfield, J. Phys. C **14**, 3795 (1981).
[18]J. E. Inglesfield and G. A. Benesh, Phys. Rev. B **37**, 6682 (1988).
[19]T. Yasuike and K. Nobusada, Phys. Rev. B **76**, 235401 (2007).
[20]T. Yasuike and K. Nobusada, Chem. Phys. Lett. **457**, 241 (2008).
[21]T. Yasuike and K. Nobusada, Phys. Rev. B **80**, 035430 (2009).
[22]P. Nordlander and J. C. Tully, Phys. Rev. B **42**, 5564 (1990).
[23]I. Panas, J. Schüle, P. Siegbahn, and U. Wahlgren, Chem. Phys. Lett. **149**, 265 (1988).
[24]K. Hermann, P. S. Bagus, and C. J. Nelin, Phys. Rev. B **35**, 9467 (1987).
[25]M. Walter, P. Frondelius, K. Honkala, and H. Häkkinen, Phys. Rev. Lett. **99**, 096102 (2007).
[26]P. S. Bagus and G. Pacchioni, Phys. Rev. B **48**, 15262 (1993).
[27]P. S. Bagus and G. Pacchioni, J. Chem. Phys. **102**, 879 (1995).
[28]P. S. Bagus, A. Wieckowski, C. Wöll, Int. J. Quantum Chem. **110**, 2844 (2010).
[29]J. R. Chelikowsky, N. Troullier, and Y. Saad, Phys. Rev. Lett. **72**, 1240 (1994).
[30]M. A. L. Marques, A. Castro, G. F. Bertsch, and A. Rubio, Comput. Phys. Commun. **151**, 60 (2003).
[31]W. Kohn and L. J. Sham, Phys. Rev. **140**, 1133 (1965).
[32]D. E. Manolopoulos, J. Chem. Phys. **117**, 9552 (2002).
[33]T. Gonzalez-Lezana, E. J. Rackham, and D. E. Manolopoulos, J. Chem. Phys. **120**, 2247 (2004).
[34]N. Moiseyev, Phys. Rep. **302**, 211 (1998).
[35]J. Taylor, H. Guo, and J. Wang, Phys. Rev. B **63**, 121104(R) (2001).
[36]M. Brandbyge, J.-L. Mozos, P. Ordejón, J. Taylor, and K. Stokbro, Phys. Rev. B **65**, 165401 (2002).
[37]M. Ernzerhof, J. Chem. Phys. **125**, 124101 (2006).
[38]T. Berggren, Phys. Lett. B **33**, 547 (1970).
[39]P. Jørgensen, J. Chem. Phys. **57**, 4884 (1972).
[40]M. E. Casida, in *Recent Advances in Density Functional Methods, Part I*, edited by D. P. Chong (Singapore, World Scientific, 1995), p. 155.
[41]S. Å. Lindgren, L. Walldén, J. Rundgren, P. Westrin, and J. Neve, Phys. Rev. B **28**, 6707 (1983).
[42]N. Troullier and J. L. Martins, Phys. Rev. B **43**, 1993 (1991).
[43]J. P. Perdew and A. Zunger, Phys. Rev. B **23**, 5048 (1981).
[44]V. Eyert, J. Comp. Phys. **124**, 271 (1996).
[45]P. E. M. Siegbahn, M. A. Nygren, and U. Wahlgren, in *Cluster Models for Surface and Bulk Phenomena*, edited by G. Pacchioni, P. S. Bagus, and F. Parmigiani, NATO ASI Series B (Plenum, New York, 1992), Vol. 283, p. 267.
[46]K. Giesen, F. Hage, F. J. Himpsel, H. J. Riess, and W. Steinmann, Phys. Rev. Lett. **55**, 300 (1985).
[47]D. Straub and F. J. Himpsel, Phys. Rev. B **33**, 2256 (1986).
[48]G. Lüpke, D. J. Bottomley, and H. M. van Driel, Phys. Rev. B **49**, 17303 (1994).
[49]T. Hertel, E. Knoesel, M. Wolf, and G. Ertl, Phys. Rev. Lett. **76**, 535 (1996).
[50]E. V. Chulkov, V. M. Silkin, and P. M. Echenique, Surf. Sci. **437**, 330 (1999).
[51]M. Bauer, S. Pawlik, and M. Aeschlimann, Phys. Rev. B **55**, 10040 (1997).
[52]M. Bauer, S. Pawlik, and M. Aeschlimann, Phys. Rev. B **60**, 5016 (1999).
[53]D. A. Arena, F. G. Curti, and R. A. Bartynski, Phys. Rev. B **56**, 15404 (1997).
[54]S. Ogawa, H. Nagano, and H. Petek, Phys. Rev. Lett. **82**, 1931 (1999).
[55]A. G. Borisov, J. P. Gauyacq, A. K. Kazansky, E. V. Chulkov, V. M. Silkin, and P. M. Echenique, Phys. Rev. Lett. **86**, 488 (2001).